Hindawi
Wireless Communications and Mobile Computing
Volume 2020, Article ID 8881436, 5 pages
https://doi.org/10.1155/2020/8881436

Research Article

Practical BER-Based Estimation of Residual OFDM CFO by Reducing Noise Margin

Ante Mihaljević,[1] Adriana Lipovac,[1] Vlatko Lipovac,[1] and Jasmin Musovic[2]

[1]*Dept. of Electrical Engineering and Computing, University of Dubrovnik, Dubrovnik, Croatia*
[2]*Communications Regulatory Agency, Sarajevo, Bosnia and Herzegovina*

Correspondence should be addressed to Adriana Lipovac; adriana.lipovac@unidu.hr

Received 27 March 2020; Revised 31 July 2020; Accepted 8 September 2020; Published 26 September 2020

Academic Editor: Minseok Kim

The main OFDM drawbacks are Carrier Frequency Offset (CFO) and large Peak-to-Average Power Ratio (PAPR), which both degrade the Bit Error Rate (BER). Specifically, we consider here clipping or any other PAPR reduction method sufficient to prevent the nonlinear high-power amplifier from generating errors. Moreover, in small cells, the signal-to-noise ratio is large, while the small time dispersion allows the OFDM symbol cyclic prefix to prevent intersymbol interference. This retains the CFO to solely determine the BER and vice versa, enabling indirect estimation of CFO-induced phase distortion by simple BER testing. However, a particular problem is measuring very low BER values (generated by alike residual CFO), which could last a long time in order to acquire statistically enough errors. The test time can be drastically reduced if the noise margin is reduced in a controllable way, by adding the interfering signal to each subcarrier at the receiver. This approach is shown to enable efficient and accurate short-term BER (and so CFO phase error) testing.

1. Introduction

Carrier Frequency Offset (CFO) and large Peak-to-Average Power Ratio (PAPR) are the immanent and dominating impairments of Orthogonal Frequency-Division Multiplexing (OFDM), degrading the Bit Error Rate (BER). Specifically, CFO that we focus here can significantly degrade the orthogonality among the subcarriers, so paving the way to Inter-Carrier Interference (ICI) and consequent carrier lock errors, which finally shrinks the effective noise margin [1–3].

Therefore, it is important to measure CFO, but the equipment needed for this purpose, such as the Vector Signal Analyzer (VSA) [4, 5], is rather complex and mostly available only at the test bench, which is not the case in many practical situations, specifically in the network operator field service environment, where VSA is often not affordable but handheld instrumentation, such as BER testers, is common and widely available.

With this regard, it is to expect that sort of CFO compensation is made, so the task is to quantify the residual CFO-caused phase error and qualify it under given conditions for a specific environment.

Specifically, we consider here that BER is determined just by the CFO, i.e., that clipping, or any other PAPR reduction method is sufficient to prevent the high-power amplifier (HPA) nonlinearity of being a significant error generating mechanism [6–11].

Moreover, in small cells, the signal is usually quite strong, implying that the signal-to-noise ratio (SNR) is large, while the evidently small time dispersion allows the OFDM symbol cyclic prefix (CP) to prevent intersymbol interference (ISI) [12]. This retains the CFO to solely determine the BER and vice versa, enabling indirect estimation of CFO by simple BER testing.

Furthermore, back to basics, the well-known BER expression for the Quadrature Amplitude Modulation (QAM) signal transmission over the additive white Gaussian noise (AWGN) channel with E_b/N_0 ratio of the energy E_b of a bit and noise spectral density N_0 is [13]:

$$\mathrm{BER} = \frac{4 \cdot Q\left(\sqrt{((3(E_b/N_0)) \cdot (\log_2 M))/M - 1}\right)}{\log_2 M}, \quad (1)$$

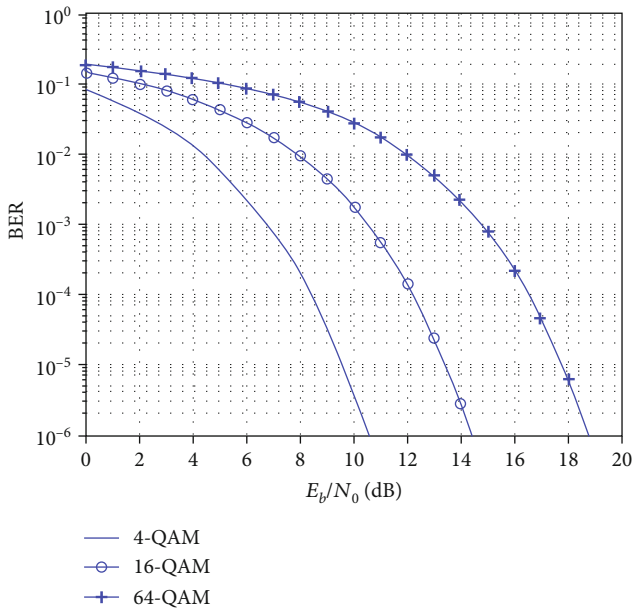

Figure 1: The waterfall BER(E_b/N_0) curves [1].

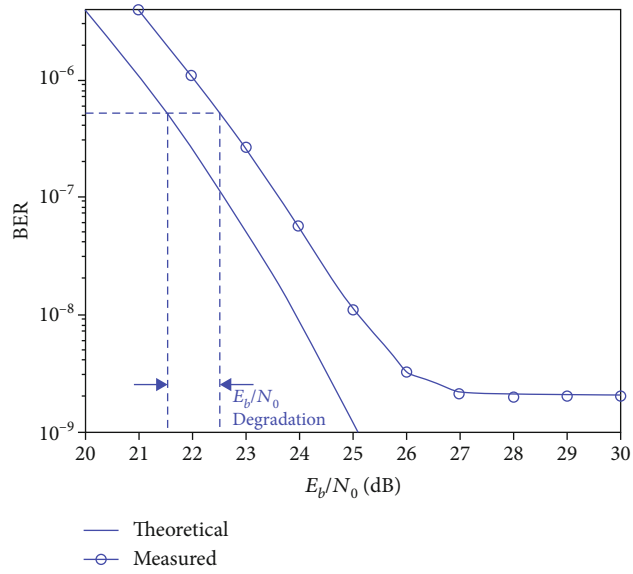

Figure 2: Measured vs. theoretical BER [2].

where Q denotes the Gaussian tail function, graphed for the three relevant modulations, in Figure 1.

Moreover, applying link abstraction principle, we can still use the above AWGN model but considering any non-AWGN distortion as an equivalent additive noise that would produce the same BER degradation. This essentially shifts the BER(E_b/N_0) curve to the right for the adequate amount of E_b/N_0, Figure 2.

With this regard is the OFDM CFO-induced lock angle error no exception, as it, too, can be considered AWGN with according E_b/N_0 to produce the same BER degradation, which is graphed in Figure 3, for the 16-QAM case.

Finally, to estimate the peak CFO-induced phase error, we use its relation with BER [3]. However, the problem arises as the so obtained BER values are very small, as the bit errors due to the residual CFO occur very rarely. Consequently, the BER test time might be excessive and the so obtained BER values inaccurate.

So, in Section 2, we complement the BER-based CFO-induced peak phase deviation prediction for the high-SNR and multipath-free common AWGN channel with the additional controllable deterministic interference signal aimed to reduce the noise margin and so enable acquisition of sufficient count of errors within a short time. In Section 3, we verify the model by means of Monte Carlo (MC) simulations, while conclusions are summarized in Section 4.

2. BER-Based Estimation of CFO-Induced Peak Phase Deviation

Recently, it has been shown how the maximal CFO-caused squared phase deviation and the instantaneous per-OFDM-symbol PAPR determine the transmission performance, essentially the BER [3]. Moreover, successful PAPR reduction (e.g., by clipping), which was shown to indirectly suppress the CFO-caused phase deviation, too [3], implies that BER degradation in this case practically remains solely determined by the CFO-induced phase deviation and vice versa.

Consequently, as BER testing is simple with respect to complex modulation signal analysis, it comes out that in many practical situations we can estimate the residual CFO from BER, applying the link abstraction method.

Essentially, the peak CFO-induced (squared) phase deviation $\Delta\Phi^2_{k\,\max}$has been shown to be related to BER as it follows [2]:

$$\Delta\Phi^2_{k\,\max}(\mathrm{BER}) \approx 30 \cdot \frac{(\Delta f_{\mathrm{CFO}} M T_s)^2}{s_k^2} \cdot \cdot \log\left(10^{\mathrm{BACK\text{-}OFF}/10} + 10^{\sqrt{3/(m-1)}\cdot\left(1/\left(Q^{-1}(\mathrm{BER}\cdot\log_2 M/4)\right)\right)/10}\right), 1 \le k \le M, \quad (2)$$

where Δf_{CFO}, M, m, and T_S are the CFO, the total number of subcarriers, the QAM modulation order, and the original (pre-OFDM) symbol duration, respectively, whereas the high-power amplifier (HPA) operating point is determined by its BACK-OFF from the nominal one (providing linear HPA operation).

2.1. Practical Small-BER Measurements. As it has been already mentioned, a particular problem here is measuring the expectedly very low BER values (reflecting the very small residual CFO), which could last for days in order to acquire statistically enough of (rare) error occurrences.

The BER test time can be drastically reduced (to a couple of minutes only), if the noise margin is reduced in a controllable way. This could be quite simply done by means of adding the interfering sinusoidal signal to each subcarrier at the receiver, before symbol detection. As it can be seen at

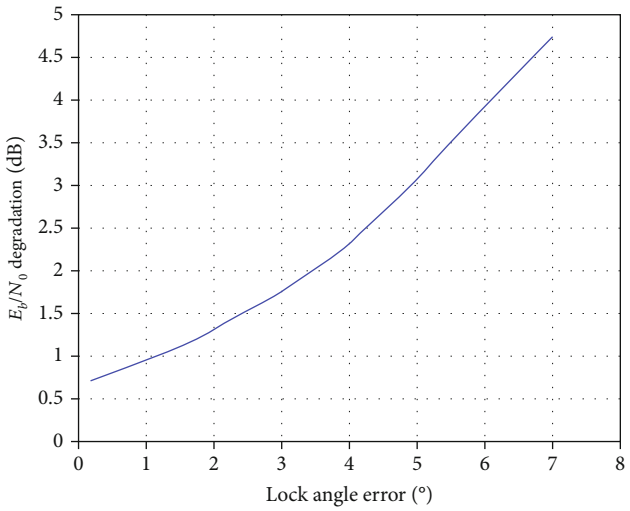

FIGURE 3: Equivalent E_b/N_0 degradation due to carrier lock angle error [2].

the practical constellation diagram presented in Figure 4, concentric circles around each 16-QAM symbol are in fact traces of the interfering vectors superimposed to symbol vectors, while rotating around them with angular speed equal to the difference between the frequencies of the subcarrier and the interferer.

As it can be seen, the symbol states are now mutually much closer so that the errors occur more frequently, which enables the short-term BER testing.

However, the question remains: How are such (increased) BER values related to the real ones?

The answer is provided by the symbol error generating model taking into account the noise and the sinusoidal interference.

Such visual effect of the sinusoidal tone on the symbol is to be modelled by considering the probability of a symbol overpassing a single decision threshold, Figure 5.

It can be seen in Figure 6 that the effective (now narrowed) noise margin is $d - I \cdot \cos\theta$, where I denotes the amplitude of the interfering signal, whose phase θ can take any value in between 0 and 2π.

In order to estimate the symbol error rate, the noise margin is normalized to the effective noise value of σ, which makes the decision threshold equal to $(d - I \cdot cos\theta)/\sigma$ so that the probability of a symbol overpassing a single decision boundary equals the corresponding Gaussian tail function:

$$\mathrm{BER} = Q\left(\frac{d - I \cdot \cos\vartheta}{\sigma}\right), \tag{3}$$

where the phase θ is expressed as the multiple n of arbitrary small angle intervals $\Delta\theta$, obtained by dividing 2π by N mutually equal parts:

$$\vartheta = \left(n - \frac{1}{2}\right) \cdot \Delta\vartheta, \Delta\vartheta = \frac{2\pi}{N}, \tag{4}$$

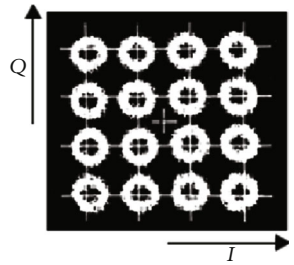

FIGURE 4: Reduced noise margin (to increase BER).

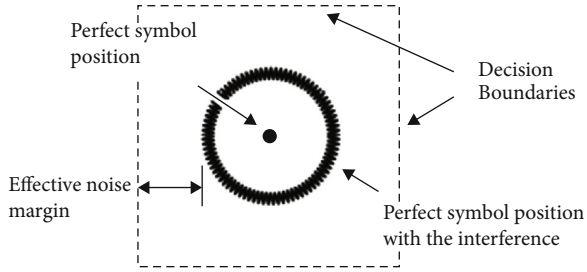

FIGURE 5: Superimposing the interfering tone with a symbol.

We consider that, for large enough N, the Gaussian tail function $Q(\cdot)$ does not significantly change within the interval $\Delta\theta$. Moreover, beside as large N as possible, the accuracy of this approximation in the middle of $\Delta\theta$ is enhanced by the shift "1/2" in the above expression.

So, by applying (4), (3) becomes the following approximation:

$$BER \approx \frac{1}{N} \cdot \sum_{n=1}^{N} Q\left[\frac{d - I \cdot \cos\left(2\pi \cdot ((n - (1/2))/N)\right)}{\sigma}\right], \tag{5}$$

where I and σ are usually expressed by carrier-to-noise C/N and carrier-to-interference C/I (in dB), respectively:

$$\begin{aligned} I &= \sqrt{2}d \cdot 10^{-C/I-K/20}, \\ \sigma &= d \cdot 10^{-C/I-K/20}. \end{aligned} \tag{6}$$

The factor K (expressed in dB) in the above equations relates the carrier power (C) and the applied modulation type. So, e.g., for 4-QAM, it is $K = 0$, while for 16-QAM, it rises to $K = 10 \cdot \log 5 = 6.99$, etc. Moreover, as (3) and (5) express BER due to signal passing a single decision boundary for various modulation types, in front of the sum in (5), coefficients should be inserted taking into account the average number of potential boundary transitions for the modulation of interest.

So, it comes out that, for the in-phase component of 16-QAM, there are two boundaries for the inner symbols, and a single boundary for the outer ones, which implies that the modulation-related factor equals 1.5. Furthermore, for QPSK and 64-QAM, it equals 2 and 1.75, respectively.

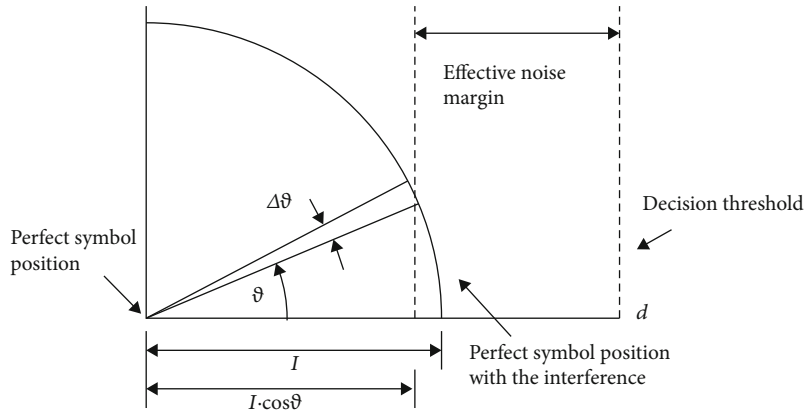

Figure 6: Symbol error mechanism due to noise and interfering tone.

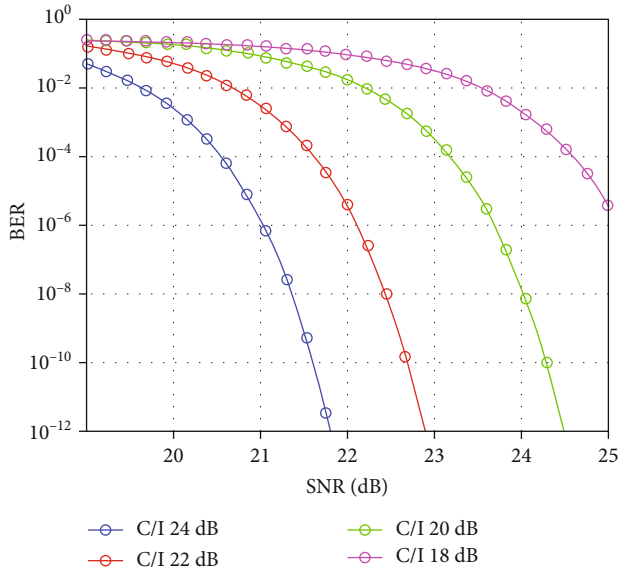

Figure 7: BER (SNR) with C/I as a parameter, 16-QAM.

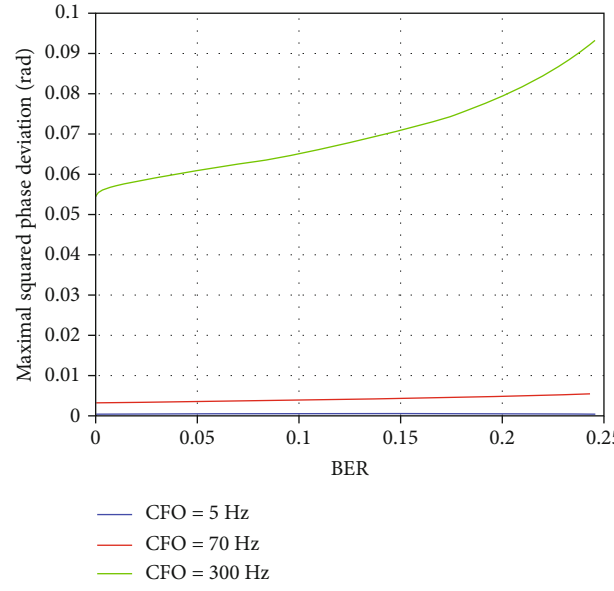

Figure 8: $\Delta\Phi^2_{k\,\max}$(BER); 5 dB HPA back-off, 16-QAM.

Based on the presented model for reducing the noise margin by introducing the narrowband deterministic radio interference, the according tabular and graphical representations of (5) can be applied in practice, such as for 16-QAM in Figure 7.

By selecting moderate levels of the interfering tone, such as say, $C/I = 18$ dB, for the exemplar $SNR = 21$ dB, the measured BER value is found to be $1.41{\cdot}10^{-1}$. Then, the corresponding residual BER at the same SNR value of 21 dB, but for much smaller interference (concretely, for C/I =24 dB), for 16-QAM, equals $1.3{\cdot}10^{-6}$, which can be seen in Figure 8, at the intersection of the vertical line at the $SNR = 21$ dB with the curves for $C/I = 18$ dB and $C/I = 24$ dB.

3. Verification

The presented CFO model applies for any back-off value, CFO level, and QAM modulation order, as these all appear in (2) as parameters. So, for our exemplar tests, where we chose 16-QAM modulation scheme, 5 dB back-off, and CFO of 300 Hz, the relationship between the residual (squared) phase deviation $\Delta\Phi^2_{k\,\max}$ and BER is presented in Table 1, resulting from (2)/(5) and MC simulations.

Accordingly, in Figure 8, the (squared) phase deviation estimation plots for the CFO values of 5, 70, and 300 Hz and the 16-QAM modulation scheme are presented.

From the above table and graphs, a very good matching is evident between the estimated and the MC simulation-based BER values for equal residual $\Delta\Phi^2_{k\,\max}$ values. This preliminary verifies the proposed model.

4. Conclusion

Estimating the OFDM CFO-induced peak phase distortion could be desirable in various situations of the radio network life cycle, from development and production of network elements and systems, to their field deployment.

Moreover, in many practical situations such as with small cells, the signal-to-noise ratio is large, and the time dispersion is small, allowing the OFDM symbol cyclic prefix to prevent

Table 1: CFO-induced peak phase deviation vs BER, 16-QAM.

	Estimation (2)/(5)	MC simulations
BER	$1.23 \cdot 10^{-1}$	$1.41 \cdot 10^{-1}$
$\Delta\Phi^2_{k\ \max}$ [rad]	0.068	0.068

intersymbol interference, so the CFO can be considered to solely determine the BER and vice versa.

So, we indirectly estimated the CFO-induced peak phase distortion by simple BER testing. However, measuring low BER values generated by alike residual CFO may not be reliable from the standpoint of statistical sufficiency of error occurrences. With this regard, we reduced the noise margin in a controllable way, by adding the interfering sinusoidal tone to each OFDM subcarrier at the receiver.

This approach is shown to enable efficient and accurate short-term BER (and so CFO phase error) prediction, which is preliminarily checked and validated by MC simulations.

Data Availability

No data were used to support this study.

Conflicts of Interest

The authors declare that there is no conflict of interest regarding the publication of this paper.

References

[1] A. Lipovac and A. Mihaljević, "BER based OFDM PAPR estimation," in *2018 26th International Conference on Software, Telecommunications and Computer Networks (SoftCOM),*, pp. 1–6, Split, Croatia, 2018.

[2] A. Lipovac, E. Škaljo, V. Lipovac, and P. Njemčević, "BER-based estimation of OFDM CFO-caused symbol phase deviation," in *2018 Advances in Wireless and Optical Communications (RTUWO)*, pp. 89–93, Riga, Latvia, 2018.

[3] A. Lipovac, V. Lipovac, and P. Njemcevic, "Suppressing the OFDM CFO-caused constellation symbol phase deviation by PAPR reduction," *Wireless Communications and Mobile Computing*, vol. 2018, Article ID 3497694, 8 pages, 2018.

[4] M. Rumnay, *LTE and the Evolution of 4G Wireless; Design and Measurements Challenges, 2nd Edition*, John Wiley & Sons, 2013.

[5] Agilent Technologies, *3GPP LTE Modulation Analysis -89600 Vector Signal Analysis Software*, Agilent Technologies, 2010.

[6] H. A. Ahmed, A. I. Sulyman, and H. S. Hassanein, "Bit error rate performance of orthogonal frequency-division multiplexing relaying systems with high power amplifiers and Doppler effects," *Wireless Communications and Mobile Computing*, vol. 13, no. 8, p. 744, 2013.

[7] T. Jiang and Y. Wu, "An overview: peak-to-average power ratio reduction techniques for OFDM signals," *IEEE Transactions on Broadcasting*, vol. 54, no. 2, pp. 257–268, 2008.

[8] S. H. Han and J. H. Lee, "Modulation, coding and signal processing for wireless communications - an overview of peak-to-average power ratio reduction techniques for multicarrier transmission," *IEEE Wireless Communications*, vol. 12, no. 2, pp. 56–65, 2005.

[9] D. Guel and J. Palicot, "Analysis and comparison of clipping techniques for OFDM peak-to-average power ration reduction," *IEEE Transactions on Broadcasting*, vol. 53, no. 3, pp. 719–724, 2007.

[10] H. Ochiai and H. Imai, "Performance analysis of deliberately clipped OFDM signals," *IEEE Transactions on Communications*, vol. 50, no. 1, pp. 89–101, 2002.

[11] S. B. Slimane, "Reducing the peak-to-average power ratio of OFDM signals through precoding," *IEEE Transactions on Vehicular Technology*, vol. 56, no. 2, pp. 686–695, 2007.

[12] A. Lipovac, V. Lipovac, and B. Modlic, "Modeling OFDM irreducible BER with impact of CP length and CFO in multipath channel with small delay dispersion," *Wireless Communications and Mobile Computing*, vol. 16, no. 9, p. 1077, 2016.

[13] A. Lipovac, B. Modlic, and M. Grgić, "OFDM error floor based EVM estimation," in *2016 24th International Conference on Software, Telecommunications and Computer Networks (SoftCOM)*, pp. 1–5, Split, Croatia, 2016.